nature medicine

Elimination of large tumors in mice by mRNA-encoded bispecific antibodies

Christiane R Stadler[1], Hayat Bähr-Mahmud[1], Leyla Celik[1], Bernhard Hebich[1,5], Alexandra S Roth[1,5], René P Roth[1,5], Katalin Karikó[1], Özlem Türeci[2] & Ugur Sahin[1,3,4]

The potential of bispecific T cell–engaging antibodies is hindered by manufacturing challenges and short serum half-life. We circumvented these limitations by treating mice with *in vitro*–transcribed pharmacologically optimized, nucleoside-modified mRNA encoding the antibody. We achieved sustained endogenous synthesis of the antibody, which eliminated advanced tumors as effectively as the corresponding purified bispecific antibody. Because manufacturing of pharmaceutical mRNA is fast, this approach could accelerate the clinical development of novel bispecific antibodies.

Bispecific T cell–engager antibodies recruit cytotoxic T cells to tumor cells and induce target-dependent polyclonal T cell activation and tumor cell lysis. Various bispecific antibody (bsAb) formats are being explored, including tandem bi-$(scFv)_2$ proteins, representing fusions of single-chain variable fragments (scFv) with different specificities[1]. A successful example is blinatumomab[2], a CD19 × CD3 bi-$(scFv)_2$ that co-clusters T cells to lymphoma cells[3] and is approved for treatment of acute lymphoblastic leukemia[4,5]. Most bsAb formats suffer from manufacturing challenges, including poor stability during long-term storage, a tendency to aggregate over time and the presence of various impurities. Consequently, manufacturing process development, production, testing and release of clinical-grade material for new bsAb drugs often requires years. Furthermore, because the serum half-life of bi-$(scFv)_2$ proteins is less than 2 h in patients, an infusion pump is required for continuous delivery[1].

We hypothesized that these limitations could be circumvented by generating bsAb *in vivo*, in the patient, using engineered mRNA[6]. To prevent immune activation, we incorporated modified nucleosides into *in vitro*–transcribed (IVT) mRNA[7–9]. Efficient translation of the modified mRNA was ensured by removing double-stranded RNA[10]. Moreover, the 5′ and 3′ UTRs and the poly(A) tail were optimized for improved intracellular stability and translational efficiency[8,11].

We generated 1-methylpseudouridine-containing mRNAs encoding His-tagged bsAbs (RiboMABs) (**Fig. 1a**) directed against the T cell receptor–associated molecule CD3 and one of three tumor-associated antigens (TAAs): the tight-junction proteins claudin 6 (CLDN6)[12,13] and claudin 18.2 (CLDN18.2)[12,14] and the epithelial cell adhesion molecule (EpCAM). We studied three bi-$(scFv)_2$ antibodies (CD3 × CLDN6, CLDN18.2 × CD3, and EpCAM × CD3), each translated from a single mRNA strand, and one Fab-$(scFv)_2$ antibody (CD3 × $(CLDN6)_2$), which required assembly of two proteins encoded by separate mRNAs. The integrity of the IVT bsAb mRNAs and RiboMABs obtained from the supernatants of K562 cells transfected with the mRNAs was confirmed (**Fig. 1b** and **Supplementary Fig. 1a,b**), and the potency of the RiboMABs was evaluated in cytotoxicity assays with human peripheral blood mononuclear cells (PBMCs) as effectors and TAA-expressing tumor cell lines as targets. The potencies of the RiboMABs and the corresponding recombinant proteins were comparable; EC_{50} (50% effective concentration; 2.6–41.6 pM) and EC_{95} (95% effective concentration; 29.8–844.5 pM) values were in the picomolar range, and maximum lysis ranged from 76–95% (**Fig. 1c** and **Supplementary Fig. 1c,d**). All RiboMABs induced dose-dependent and target-specific T cell activation and target lysis, even at concentrations (1.9 nM) far above the EC_{95} (**Fig. 1d** and **Supplementary Fig. 1e**).

To evaluate whether RiboMABs generated *in vivo* in mice show therapeutic efficacy equivalent to that of their recombinant antibody counterparts, we focused on the bi-$(scFv)_2$ format, which is the most commonly used bsAb format. We formulated CD3 × CLDN6 mRNA with a polymer/lipid-based transfection reagent to ensure abundant translation in the liver after intravenous (i.v.) administration (**Supplementary Fig. 2**). Plasma levels of CD3 × CLDN6 RiboMAB endogenously translated from the administered mRNA peaked within 6 h and were sustained over several days (**Fig. 2a**, right). Accordingly, the *ex vivo* cytotoxic activity of plasma from the treated mice exerted a maximum lysis of 90% at 6 h and remained above the half-maximal level for up to 6 d after injection (**Fig. 2a**, left). The peak plasma concentration and *ex vivo* cytotoxic activity of RiboMAB achieved with a single dose of 5 µg of CD3 × CLDN6 mRNA were comparable to those measured following injection with 4–7 µg (200 µg per kg body weight) recombinant CD3 × CLDN6 (rCD3 × CLDN6) protein[15]. However, because of the short plasma half-life of bi-$(scFv)_2$, the levels of rCD3 × CLDN6 protein and the cytotoxic activity of the plasma dropped sharply within 6 h and were barely detectable after 24 h. In contrast, the CD3 × CLDN6 RiboMAB–mediated cytotoxicity was maintained by weekly administration of the coding mRNA (**Supplementary Fig. 3**). Of note, injection with only 0.05 µg of CD3 × CLDN6 mRNA still resulted in strong and sustained *ex vivo* cytotoxic activity (**Fig. 2b**).

After demonstrating that pharmacologically active levels of functional bi-$(scFv)_2$ protein can be achieved by i.v. administration of the corresponding coding mRNA, we investigated the therapeutic effect of two RiboMABs, CD3 × CLDN6 and EpCAM × CD3, in NSG mice engrafted with human PBMCs; these mice had also been engrafted with subcutaneous

[1]BioNTech, Mainz, Germany. [2]Cluster of Individualized Immunointervention (CI3), Mainz, Germany. [3]Department of Internal Medicine III, Johannes Gutenberg University, Mainz, Germany. [4]TRON–Translational Oncology at the University Medical Center of the Johannes Gutenberg University, Mainz, Germany. [5]These authors contributed equally to this work. Correspondence should be addressed to U.S. (sahin@uni-mainz.de).

Received 20 December 2016; accepted 16 May 2017; published online 12 June 2017; corrected after print 20 July 2017; doi:10.1038/nm.4356

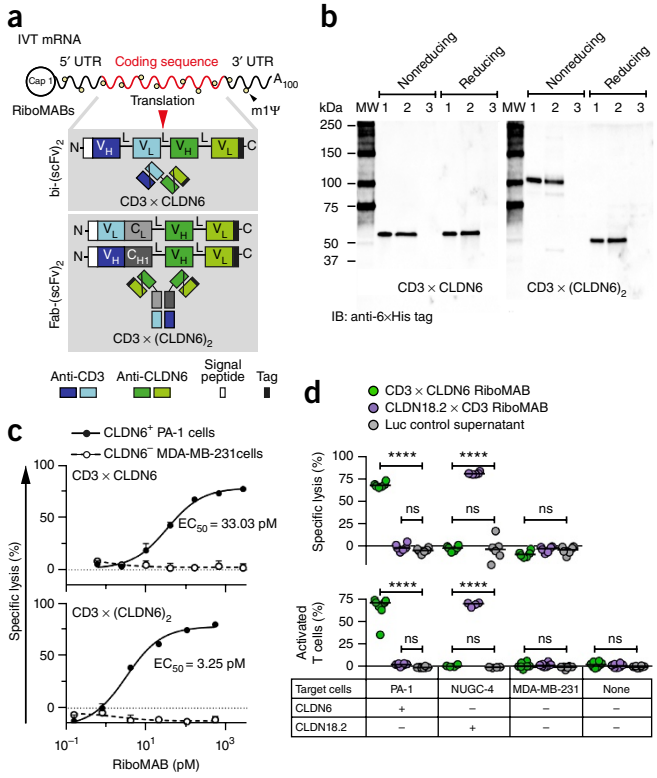

Figure 1 *In vitro* target-dependent lysis of human tumor cell lines by picomolar amounts of *in vitro*–transcribed mRNA encoding T cell–engager bispecific antibodies. (**a**) Structures of the IVT bi-$(scFv)_2$ and Fab-$(scFv)_2$ RiboMABs. (**b**) Immunoblot detection with a horseradish peroxidase (HRP)-conjugated antibody to 6×His of two representative His-tagged RiboMABs in supernatants from K562 producer cells (lane 2). Positive control (lane 1), 20 ng of the corresponding purified recombinant protein; negative control (lane 3), supernatant from mock-electroporated K562 cells. The experiment was repeated four times. (**c**,**d**) Target-specific lysis and T cell activation by CLDN6- or CLDN18.2-specific RiboMAB. Bulk human PBMCs and CLDN6-positive (PA-1), CLDN18.2-positive (NUGC-4) or double-negative (MDA-MB-231) luciferase (Luc)-transduced human tumor cell lines (effector:target ratio of 5:1) were co-cultured for 48 h with supernatants from the RiboMAB-secreting K562 producer cell line. (**c**) Specific lysis of PA-1 cells by bi-$(scFv)_2$ (top) and Fab-$(scFv)_2$ (bottom) RiboMAB. Mean values from three technical replicates are shown with s.d. (**d**) Top, specific lysis was assessed via a luciferase-based cytotoxicity assay. Bottom, target-dependent T cell activation was quantified by flow cytometry. The percentage of activated ($CD69^+CD25^-$, $CD69^+CD25^+$ or $CD69^-CD25^+$) T cells among viable, singlet $CD5^+$ lymphocytes normalized to mock-treated cells (supernatant from water-electroporated K562 cells) is shown. Control, PBMCs without target cells. 1.9 nM bi-$(scFv)_2$ RiboMAB, as determined by ELISA, was applied. Significance was evaluated by two-way ANOVA combined with Tukey's multiple-comparisons test: $^{****}P < 0.0001$ (F value (DFn, DFd) = 182.9 (2, 45)) (top) and $^{****}P < 0.0001$ (F value (DFn, DFd) = 723.9 (3, 36)) (bottom); ns, $P \geq 0.05$. Data are shown as a dot plot of 4–8 sample points from two experiments with the median. Experiments in **c** and **d** were repeated three times. A, adenylate; bi-$(scFv)_2$, bispecific single-chain variable fragment; C, C terminus; C_{H1}, constant heavy chain 1; C_L, constant light chain1; DF, degrees of freedom; EC_{50}, 50% effective concentration; E:T, effector:target ratio; Fab, fragment, antibody binding; IB, immunoblot; L, linker; m1Ψ, 1-methylpseudouridine; MW, molecular weight marker; N, N terminus; ns, not significant; V_H, variable heavy chain; V_L, variable light chain; WT, wild type.

human ovarian carcinoma xenografts. First, CD3 × CLDN6 RiboMAB was evaluated in mice bearing OV-90 tumors with an average size of 200–300 mm^3. In all mice injected once a week for three consecutive weeks with 3 µg (6 pmol) of CD3 × CLDN6 mRNA, the established OV-90 tumors were completely eliminated, whereas in control mice treated with luciferase-encoding mRNA all tumors progressed (**Fig. 2c**). To attain a comparable antitumor effect, rCD3 × CLDN6 protein had to be administered three times a week for a total of ten doses of 200 µg per kg body weight (**Fig. 2c**). In a similar experiment, tumors were collected as soon as reduction occurred. Tumors from mice injected with CD3 × CLDN6 mRNA, but not with control mRNA, were strongly infiltrated with T cells, indicating an effective concentration of bi-$(scFv)_2$ RiboMAB in the tumor tissue upon i.v. application of the mRNA (**Fig. 2d**). Of note, T cell infiltration varied in tumor layers originating from distant areas, with higher infiltration in the tumor center.

The potent antitumor efficacy of CD3 × CLDN6 RiboMAB was confirmed in NSG mice bearing subcutaneous xenografts of ES-2 ovarian carcinoma cells stably transfected to express CLDN6. The CLDN6-negative wild-type ES-2 xenografts were not affected by CD3 × CLDN6 mRNA treatment, proving evidence of strict target antigen specificity (**Fig. 2e**). To evaluate the universal applicability of the RiboMABs, we used EpCAM × CD3 IVT mRNA encoding bi-$(scFv)_2$ antibody targeting EpCAM, another TAA expressed on OV-90 tumors. Treatment of mice with EpCAM × CD3 IVT mRNA resulted in complete tumor regression (**Supplementary Fig. 4a**), thus supporting the potential of this approach.

We also evaluated bi-$(scFv)_2$-encoding IVT mRNA for safety. We detected no systemic release of proinflammatory cytokines from human PBMCs in engrafted NSG mice (**Supplementary Figs. 4b** and **5a**), indicating a lack of nonspecific T cell activation. In addition, no evidence for liver toxicity was observed (**Supplementary Fig. 5b**). Notably, when immunocompetent mice were injected with conventional CD3 × CLDN6 mRNA, which did not contain modified nucleosides and was not purified, we detected cytokines but minimal RiboMAB protein (**Supplementary Fig. 5c**). In contrast, the non-immunogenic CD3 × CLDN6 mRNA, used throughout the presented experiments, elicited no cytokines and was efficiently translated, thus confirming the importance of using purified and nucleoside-modified mRNA to generate RiboMABs.

In summary, our data show that systemic transfer of mRNAs encoding bsAbs at a low dose results in sustained production of therapeutic levels of RiboMABs with half-lives in the range of those for naturally produced immunoglobulin proteins. Repeated administration of mRNA is feasible and results in reproducible RiboMAB pharmacology, providing a sound basis for the development of clinically applicable dosing regimens.

METHODS

Methods, including statements of data availability and any associated accession codes and references, are available in the online version of the paper.

Note: Any Supplementary Information and Source Data files are available in the online version of the paper.

ACKNOWLEDGMENTS

We wish to thank the following colleagues: S. Wöll, S. Kühne and M. Erdeljan for immunohistochemistry and data acquisition, N. Brüne for clinical chemistry data, A. Jendretzki, M. LeGall and S. Wessel for construct design and preparation, and K. Schmoldt for performing the *in vitro* assays. We would also like to acknowledge I. Biermann for supporting the *in vivo* studies, H. Muramatsu, M. Baiersdörfer, K. Beilstein, S. Fesser and team for IVT mRNA synthesis and characterization and for bioluminescence studies, T. Beissert and team for cell line transduction and K. Reuter for advice on *in vivo* experiments. Special thanks are given to C. Huber for inspiring discussions.

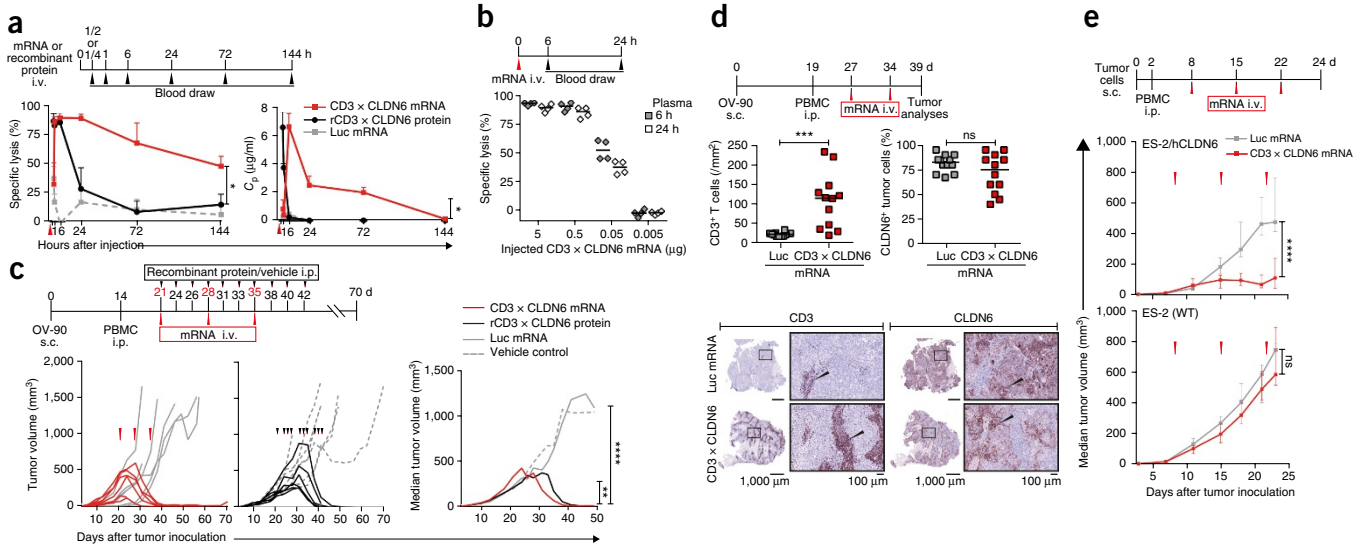

Figure 2 Sustained plasma level of functional bi-$(scFv)_2$ protein and elimination of advanced xenograft tumors upon treatment of mice with picomolar amounts of bsAb-encoding *in vitro*–transcribed mRNA. (**a**) *Ex vivo* cytotoxicity (left) and concentration (C_p) (right) of endogenously translated CD3 × CLDN6 RiboMAB in the plasma of NSG mice after i.v. administration of polymer/lipid-formulated mRNA. Mice were treated with 5 µg of CD3 × CLDN6 mRNA ($n = 5$), luciferase (Luc) mRNA control ($n = 3$) or 200 µg per kg body weight purified recombinant CD3 × CLDN6 (rCD3 × CLDN6) protein ($n = 5$). For cytotoxicity assays, PA-1 cells and human PBMCs (E:T = 5:1) were co-cultured with 5% plasma per 100 µl of total assay volume. Concentrations from technical ELISA duplicates are shown. Data are presented as means ± s.d. A two-tailed Mann–Whitney *U* test was used for analysis of significance over time: $^{*}P < 0.03$. (**b**) *Ex vivo* cytotoxicity of endogenously translated CD3 × CLDN6 RiboMAB in the plasma of NSG mice after i.v. administration of mRNA. Mice were treated with decreasing amounts of CD3 × CLDN6 mRNA ($n = 4$). PA-1 cells and human PBMCs (E:T = 5:1) were co-cultured with 1% plasma per 100 µl of total assay volume. Data are shown as a dot plot with medians. (**c**–**e**) Effect of repeated i.v. doses of CD3 × CLDN6 mRNA in NSG mice engrafted with human PBMCs and bearing advanced subcutaneous (s.c.) OV-90 or ES-2 tumor xenografts (mean tumor volume at start of treatment 200–300 mm^3 and 6–16 mm^3, respectively). (**c**) Mice were treated with CD3 × CLDN6 or luciferase mRNA ($n = 6$/group; three doses of 3 µg/mouse i.v. weekly) or with purified rCD3 × CLDN6 protein (200 µg per kg body weight) or vehicle ($n = 7$/group; three doses intraperitoneally (i.p.) weekly, total of ten doses). Tumor growth for individual mice (left, mRNA; middle, recombinant protein) and median tumor growth per group (right) are shown. Significance was evaluated by parametric two-way ANOVA: $^{****}P < 0.0001$ (*F* value (DFn, DFd) = 84.6 (3, 309)), $^{**}P = 0.0022$ (*F* value (DFn, DFd) = 9.7 (1, 150)). The experiment was conducted twice. (**d**) Mice were treated with two doses of CD3 × CLDN6 mRNA ($n = 4$) or luciferase mRNA as negative control ($n = 4$) (both 3 µg/mouse i.v. weekly). Tumor-infiltrating lymphocytes (human $CD3^+$ cells; left) and CLDN6-expressing tumor cells (right) were quantified by immunohistochemistry (IHC) in three consecutive tumor sections (median of $n = 12$ with three sections from each of the four mice). Significance was evaluated by unpaired two-tailed *t* test: $^{***}P = 0.0003$ (*t* value = 4.2, DF = 22); ns, $P = 0.1176$ (*t* value = 1.6, DF = 22). Bottom, representative IHC images (magnification, ×5). Arrowheads indicate positive staining. (**e**) Mice with ES-2 ovarian cancer xenografts transfected to express CLDN6 (ES-2/hCLDN6) or CLDN6-negative wild-type ES-2 xenografts (WT) were treated weekly with a total of three doses of 5 µg of CD3 × CLDN6 mRNA ($n = 6$) or luciferase mRNA ($n = 5$ and $n = 7$, respectively). The median with the interquartile range (whiskers) is shown for each group. Significance was evaluated by parametric two-way ANOVA: $^{****}P < 0.0001$ (*F* value (DFn, DFd) = 77.0 (1, 62)); ns, $P = 0.376$ (*F* value (DFn, DFd) = 0.8 (1, 77)). Red arrowheads indicate formulated mRNA injections (**a**–**e**). Black arrowheads indicate blood draw time points (**a**,**b**) or recombinant protein or vehicle injections (**c**).

AUTHOR CONTRIBUTIONS

C.R.S., H.B.-M., L.C., K.K., Ö.T. and U.S. were engaged in study conception and interpretation and contributed to the critical revision of the manuscript. C.R.S. designed the study and participated in *in vivo* experiment execution and in general data analysis and interpretation. H.B.-M. was involved in study design, especially of *in vitro* experiments, and in data analysis and interpretation. L.C. designed, executed and interpreted immunoblot analyses and performed recombinant protein purification. B.H. established, executed and interpreted ELISA assays and performed *in vitro* experiments. A.S.R. was involved in *in vitro* assay design, execution and interpretation and produced recombinant proteins as well as RiboMAB supernatants. R.P.R. performed *in vivo* experiments and supported the design of the studies. Ö.T., C.R.S., H.B.-M., K.K. and U.S. drafted the manuscript. All authors discussed the results, assisted in the preparation of the manuscript and approved the final version.

COMPETING FINANCIAL INTERESTS

The authors declare competing financial interests: details are available in the online version of the paper.

1. Garber, K. *Nat. Rev. Drug Discov.* **13**, 799–801 (2014).
2. Kantarjian, H. *et al. N. Engl. J. Med.* **376**, 836–847 (2017).
3. Bargou, R. *et al. Science* **321**, 974–977 (2008).
4. Spiess, C., Zhai, Q. & Carter, P.J. *Mol. Immunol.* **67** (2 Pt. A), 95–106 (2015).
5. Topp, M.S. *et al. J. Clin. Oncol.* **29**, 2493–2498 (2011).
6. Sahin, U., Karikó, K. & Türeci, Ö. *Nat. Rev. Drug Discov.* **13**, 759–780 (2014).
7. Karikó, K., Buckstein, M., Ni, H. & Weissman, D. *Immunity* **23**, 165–175 (2005).
8. Karikó, K. *et al. Mol. Ther.* **16**, 1833–1840 (2008).
9. Anderson, B.R. *et al. Nucleic Acids Res.* **38**, 5884–5892 (2010).
10. Karikó, K., Muramatsu, H., Ludwig, J. & Weissman, D. *Nucleic Acids Res.* **39**, e142 (2011).
11. Holtkamp, S. *et al. Blood* **108**, 4009–4017 (2006).
12. Micke, P. *et al. Int. J. Cancer* **135**, 2206–2214 (2014).
13. Schuler, M. *et al. Ann. Oncol.* **27**, 207–242 (2016).
14. Sahin, U. *et al. Clin. Cancer Res.* **14**, 7624–7634 (2008).
15. Stadler, C.R. *et al. OncoImmunology* **5**, e1091555 (2015).

ONLINE METHODS

Mice. Immunodeficient male and female NOD.Cg-Prkd^{scid} IL2rg^{tm1Wjl}/SzJ (NSG) mice (Jackson Laboratory, Charles River) were aged 6–18 weeks and had a body weight of 18–36 g. Female BALB/cJRj mice (aged 6–12 weeks) were purchased from Janvier Labs and had a body weight of 23–26 g. Group sizes were defined to balance statistical power estimated from previous experiments, feasibility and ethical aspects. All animal studies were approved by the local authority of Rhineland-Palatinate for the Ethical Evaluation of Animal Experiments and Animal Welfare. All mice were kept or bred in accordance with federal and state policies on animal research at the University of Mainz and BioNTech.

Cells and cell culture. Human tumor cell lines were used as TAA-positive target cells: PA-1 (CLDN6 positive, ovarian teratocarcinoma; ATCC, CRL-1572), OV-90 (CLDN6 and EpCAM positive, ovarian adenocarcinoma; ATCC, CRL-11732), ES-2 (stably CLDN6 transfected, ovarian clear cell carcinoma; ATCC, CRL-1978) and NUGC-4 (stably CLDN18.2 transduced, gastric adenocarcinoma; JCRB0834). The following cell lines were used as TAA-negative controls: MDA-MB-231 (breast adenocarcinoma; PerkinElmer, parental source ATCC, HTB-26), Raji (Burkitt's lymphoma; ATCC, CCL-86) and ES-2 (ovarian clear cell carcinoma; ATCC, CRL-1978). Expi293 (Thermo Fisher Scientific, Expression System Kit, A14635) and/or HEK-293 (ATCC, CRL-1573) cells were used for recombinant protein expression (rCD3 × CLDN6, rCD3 × $(CLDN6)_2$, rCLDN18.2 × CD3, and rEpCAM × CD3).

Cell lines were lentivirally transduced with firefly luciferase for luminescence-based cytotoxicity assays. The human chronic myelogenous leukemia cell line K562 (ATCC, CCL-243) served as the producer line for RiboMABs.

Cell lines were cultured according to the provider's recommendations and tested for mycoplasma every 3 months. Master and working cell banks were generated, and third and fourth passages were used for tumor experiments. Cell lines were authenticated by STR/DNA profiling by Eurofins in 2015 and/or ATCC in 2016.

Human PBMCs isolated from the buffy coats of healthy donors by Ficoll density-gradient centrifugation were used either in bulk or enriched for T cells by magnetic bead separation as effector cells (Pan T Cell Kit II, Human (Miltenyi)).

Cloning of template vectors and *in vitro* transcription of mRNA. Human codon-optimized DNA sequences were generated by gene synthesis (GeneArt/Thermo Fisher, Eurofins). V_H and V_L sequences for the anti-CLDN moieties were derived from previously published anti-CLDN6 IMAB027 and anti-CLDN18.2 IMAB362 full IgG antibody sequences[16,17]. Sequences for the anti-hEpCAM V_H and V_L domain, a humanized variant of 323/A3 (ref. 18), and the anti-CD3ε V_H and V_L sequences of TR66 (refs. 19,20) are published elsewhere. The variable domains of the bi-$(scFv)_2$ proteins were fused via a 15- to 25-residue glycine–serine (GS) linker. Their anti-TAA and anti-CD3ε scFv sequences were linked by a six-residue GS linker. All bi-$(scFv)_2$ constructs contained a secretion signal and a C-terminal 6×His tag. The full EpCAM × CD3 nucleotide sequence is shown below. The CD3 × $(CLDN6)_2$ Fab-$(scFv)_2$ antibody is based on the assembly of two constructs: (i) sec-V_L(anti-CD3ε)-C_L-scFv(anti-CLDN6)-6×His tag and (ii) sec-V_H(anti-CD3ε)-C_{H1}-scFv(anti-CLDN6)-Strep tag. Constant (C) domains were derived from conserved human IgG_1 sequences (IMGT). Two point mutations were introduced into the anti-CLDN6 scFv-encoding regions to allow additional stabilizing disulfide bridges (V_H(N49C) and V_L(G120C), according to IMGT numbering).

The sequences encoding bsAbs or firefly luciferase were subcloned into the multiple-cloning site (MCS) of pST1-TEV-MCS-F-I-A30LA70 (pST1)[11]. The 5′ UTR (TEV)[8,21] and 3′ UTR (F-I) of this construct have been shown to enhance stability and translation efficiency, as has the 100-nucleotide poly(A) tail interrupted by a short linker ($A_{30}LA_{70}$, where L = GCAUAUGACU)[22]. The corresponding DNA sequences in order are shown for the EpCAM × CD3 mRNA sequence as an example: 5′ UTR (TEV): TCTCAACACAACATATACAAAACAAAC GAATCTCAAGCAATCAAGCATTCTACTTCTATTGCAGCAATTTAAAT CATTTCTTTTAAAGCAAAAGCAATTTTCTGAAAATTTTCACCATTTA CGAACGATAGC, secretion signal: atgggctggtcctgcatcatcttgttcttggtggctact-gccactggagtacacagc , V_L (anti-EpCAM): GAGATTGTCCTTACACAGTCACC AGGCACCCTTTCCTTGTCTCCTGGGGAACGAGCCACCCTCAGTTGT CGGTCAAGCAAGAATCTGCTGCATTCCAATGGGATCACATACCTGTA TTGGTACCAGCAGAAGCCTGGACAGGCACCCAGACTGCTCATCTAC CAGATGTCCAATCTGGCCTCAGGCATTCCTGACAGGTTTTCCGGCA GCGGGTCTGGCACCGATTTCACCCTGACCATATCCAGGCTCGAACC AGAGGATTTTGCCGTGTATTACTGCGCACAGAATCTGGAGATTCCC CGCACTTTTGGCCAAGGGACTAAACTGGAGATCAAGCGG, linker: ggag-gaggcggctctggaggtggcggcagtggtggaggcgggtctggcggtggcggatctggaggtggtgggagc, V_H (anti-EpCAM): CAGGTCCAGCTTGTTCAGTCAGGCGCAGAGGTGAA GAAACCCGGAGCTAGCGTGAAAGTCTCCTGCAAAGCGTCAGGGTACA CCTTCACCAACTATGGGATGAACTGGGTACGTCAAGCCCCAGGGCAA AGACTCGAATGGATGGGTTGGATCAACACGTACACAGGGGAACCGAC TTATGGCGAGGACTTCAAGGGGAGAGTGACCATAACACTGGACACAT CCGCTAGCACAGCGTATATGGAGCTGAGCAGTCTGAGGAGCGAAGAT ACGGCTGTTTACTATTGTGCCCGCTTTGGTAACTACGTGGACTATTGG GGTCAGGGAACTCTGGTGACGGTTTCTAGC, linker: agtggcggcggaggatcc, V_H (anti-CD3): CAGGTGCAGCTGCAGCAGTCTGGCGCTGAGCTGGC TAGACCTGGCGCCTCCGTGAAGATGTCCTGCAAGACCTCCGGCTA CACCTTCACCCGGTACACCATGCACTGGGTCAAGCAGAGGCCTGG ACAGGGCCTGGAATGGATCGGCTACATCAACCCCTCCCGGGGCTA CACCAACTACAACCAGAAGTTCAAGGACAAGGCCACCCTGACAAC CGACAAGTCCTCCTCCACCGCCTACATGCAGCTGTCCTCCCTGACC TCCGAGGACTCCGCCGTGTACTACTGCGCCCGGTACTACGACGAC CACTACTCCCTGGACTACTGGGGCCAGGGCACCACACTGACAGTG TCTAGC, linker: ggaggcggaggatctggtggtggcggatctggcggcggtggaagtggcggag-gtggtagc, V_L (anti-CD3): CAGATCGTGCTGACCCAGTCTCCCGCCATC ATGTCTGCTAGCCCTGGCGAGAAAGTGACAATGACCTGCCGGGCC TCCTCCTCCGTGTCCTACATGAACTGGTATCAGCAGAAGTCCGGC ACCTCCCCCAAGCGGTGGATCTACGACACCTCCAAGGTGGCCTCT GGCGTGCCCTACAGATTCTCCGGCTCTGGCTCTGGCACCTCCTAC AGCCTGACCATCTCCAGCATGGAAGCCGAGGATGCCGCCACCTAC TACTGCCAGCAGTGGTCCTCCAACCCCCTGACCTTTGGCGCTGGC ACCAAGCTGGAACTGAAG, spacer: GGCGGCTCT, 6×His tag: caccac-caccatcaccac, spacer: TGATGAGCTGCAGAATTCGTCGACGGATCCGAT, 3′ UTR (F-I): CTGGTACTGCATGCACGCAATGCTAGCTGCCCCTTTCCCG TCCTGGGTACCCCGAGTCTCCCCCGACCTCGGGTCCCAGGTATGCTC CCACCTCCACCTGCCCCACTCACCACCTCTGCTAGTTCCAGACACCTC CCAAGCACGCAGCAATGCAGCTCAAAACGCTTAGCCTAGCCACACCC CCACGGGAAACAGCAGTGATTAACCTTTAGCAATAAACGAAAGTTTAA CTAAGCTATACTAACCCCAGGGTTGGTCAATTTCGTGCCAGCCACACC, spacer: CTCGAGCTAGC, poly(A) tail (A_{30}): aaaaaaaaaaaaaaaaaaaaaaaaaaaaaa, poly(A) tail linker: gcatatgact, poly(A) tail (A_{70}): aaaaaaaaaaaaaaaaaaaaaaaaaa aaaaaaaaaaaaaaaaaaaaaaaaaaaaaaaaaaaaaaaaaa.

The plasmids were linearized with SapI and served as the template for mRNA IVT using T7 RNA polymerase and a transcription kit (MegaScript, Ambion). The UTP in the reaction was replaced with 1-methylpseudouridine triphosphate (N^1-methylpseudouridine-5′-triphosphate, m1ΨTP) (TriLink)[10]. m^7G5′ppp5′G2′-O-Met-capped (cap1) IVT mRNAs were generated using vaccinia virus guanylyltransferase and 2′-O-methyltransferase (NEB).

Upon IVT mRNA production, single-stranded RNA was enriched by HPLC purification and the absence of double-stranded RNA (dsRNA) was confirmed using the dsRNA-specific mAb J2 (10010200, English and Scientific Consulting) as described elsewhere[10]. The concentration and quality of the purified dsRNA-free IVT mRNA were assessed by spectrophotometry on a 2100 Bioanalyzer (Agilent), and the mRNA was stored at –20 °C.

Polymer/lipid-based formulation of mRNA. For i.v. administration in *in vivo* studies, mRNA was formulated with the TransIT-mRNA Transfection kit (Mirus Bio). Five micrograms of mRNA in 190 µl of cold DMEM with 4.5 g/l glucose (Thermo Fisher) was mixed with 5.6 µl of TransIT-mRNA reagent and 3.6 µl of TransIT Boost reagent. mRNA reactions were immediately vortexed, incubated at room temperature for 2 min and injected into mice within 5 min. The total volume for 0.005–5 µg of mRNA complex was 200 µl.

ELISA quantification of RiboMABs. For detection of bi-$(scFv)_2$ antibody, MaxiSorp plates (Thermo Scientific) were coated overnight at 4 °C with a

doi:10.1038/nm.4356

mouse anti-idiotype antibody to capture the CD3 scFv region, washed with 0.05% Tween-20 in PBS, and blocked at room temperature with 3% BSA in PBS for 2 h. A serial dilution of the corresponding purified recombinant CD3 × TAA or TAA × CD3 protein as a concentration standard and K562 producer cell supernatants or NSG mouse plasma diluted in 0.2% BSA in PBS were added to the coated plates as replicates for 2 h at room temperature. For detection, polyclonal (1:5,000; ab1187, Abcam) or monoclonal (clone GG11-8F3.5.1; 1:625; 130-092-783, Miltenyi) anti-6×His-HRP antibody was added in 0.2% BSA in PBS and plates were incubated for 1 h at room temperature. Plates were incubated with TMB substrate solution (Kem-En-Tec) at room temperature in the dark for 15 min, and the reaction was stopped bythe addition of 2.5% H_2SO_4. Analysis was conducted on a Tecan M200 microplate reader at 450 and 620 nm.

For detection of Fab-$(scFv)_2$ antibody in K562 producer cell supernatants, a goat anti–human IgG F(ab′)$_2$ antibody (STAR126, AbD Serotec) was coated onto MaxiSorp plates (Thermo Scientific) at 37 °C for 1 h and plates were blocked with 3% milk at 4 °C overnight. After washing (0.05% Tween-20 in PBS), dilution rows of purified rCD3 × $(CLDN6)_2$ protein as a concentration standard and K562 supernatants were added. Next, 100 µl of mouse anti-idiotype antibody (3.5 µg/ml; clone 4G10, Ganymed) was added to capture the CLDN6 scFv regions of the Fab-$(scFv)_2$ protein and plates were incubated for 1 h at room temperature. For detection, a polyclonal AP-conjugated goat anti–mouse IgG (Fc) antibody (1:500; 115-055-062, Jackson ImmunoResearch) was used. Plates were incubated with 100 µl of pNPP substrate solution (PanReac AppliChem) at room temperature in the dark for 30 min, and the reaction was stopped by the addition of 100 µl of 3 M KOH. Analysis was conducted on a Tecan M200 microplate-reader at 405 and 492 nm.

bsAbs were quantified in technical triplicates (K562 supernatants) or duplicates (mouse plasma).

RiboMAB expression in human cell lines. Cells were suspended in ice-cold X-VIVO 15 (Lonza) and mixed with bsAb-encoding IVT mRNA or water as a control (mock) in a 0.4-cm Gene Pulser/MicroPulse electroporation cuvette (Bio-Rad). Electroporation was performed with the GenePulser MXcell System (Bio-Rad) under the following conditions: K562 cells: 4×10^6 cells/ml, 200 V, 8 ms, 3 pulses; PA-1 cells: 1×10^7 cells/ml, 200 V, 12 ms, 2 pulses. Cells were placed on ice, counted and analyzed for viability. For production of RiboMABs, K562 cells were electroporated 48 h before the assay with 25 µg/ml bi-$(scFv)_2$ mRNA or 25 µg/ml of each Fab-$(scFv)_2$ mRNA (1:1 ratio of the IVT mRNAs) and seeded into complete culture medium at a density of 5×10^5 cell/ml in six-well tissue culture plates. Supernatant was collected after 48 h by centrifugation and sterile filtered (0.2-µm Minisart NML syringe filters (Sartorius)). PA-1 target cells electroporated with 20 µg/ml mRNA were seeded directly after viability analysis.

Recombinant protein expression and purification. rCD3 × CLDN6 bi-$(scFv)_2$ protein was expressed in HEK-293 cells[15] and all other recombinant bsAbs were expressed with the Expi293 expression system (Thermo Fisher Scientific) according to the manufacturer's instructions. bsAb culture supernatants collected from producer cell lines were subjected to immobilized metal affinity chromatography (IMAC) and size exclusion chromatography (GE Healthcare Life Sciences). Eluted proteins were dialyzed against vehicle buffer consisting of 10 mM NaOAc (Carl Roth) in water, pH 5.5, or against DPBS, pH 7.4.

Immunoblot analysis. 20 µl of supernatant from K562 producer cells was heated to 95 °C for 10 min in Laemmli buffer with (reducing) or without (non-reducing) 1 M dithiothreitol (DTT; final concentration 0.1 M). Supernatants and purified recombinant bsAbs were separated by polyacrylamid gel electrophoresis (4–15% Criterion TGX Stain-Free Gel (Bio-Rad)), followed by immunoblot analysis and visualization with an HRP-conjugated polyclonal anti–6×His tag antibody (1:10,000; ab1187, Abcam).

Cytotoxicity assays. 5×10^4 human PBMCs as effector cells were plated together with 1×10^4 luciferase-transduced target cells into white 96-well flat-bottom plates (Nunc). K562 supernatant containing RiboMABs was added in a dilution row to the experimental lysis samples (L_{exp}) and mock supernatant from water-electroporated K562 cells was added to the minimum lysis (L_{min}) and maximum lysis (L_{max}) control wells, all in triplicate. Dilution rows and single concentrations were prepared with mock supernatant as the diluent. Plates were incubated for 48 h before lysis of L_{max} cells with Triton X-100 and addition of a buffered luciferin solution (BD Monolight luciferin, BD Biosciences).

Data were analyzed by a sigmoidal dose-response (standard slope) algorithm, and the means of at least three replicates with s.d. were calculated. Cytotoxicity assays were repeated at least three times.

T cell activation. 2.5×10^5 PBMCs were plated alone or together with 5×10^4 target cells into transparent 24-well plates (Nunc). K562 supernatant containing RiboMABs was added at a concentration of 1.9 nM. OKT3 (BE0001-2, BioXCell) at a concentration of 200 ng/ml (~1.3 nM) was used as a target-independent T cell activation control for PBMCs only. Effector cell–containing supernatant (incubated for 48 h) was collected , and effector cells were resuspended in FACS buffer (2% FBS in DPBS) supplemented with the fluorescin-conjugated anti-human antibodies anti-CD5-PE-Cy7 (clone UCHT2; ab155375, Abcam), anti-CD25-PE (clone M-A251; 555432, BD Biosciences) and anti-CD69-APC (clone L78; 340560, BD Biosciences) and the viability dye eFluor506 (eBioscience). Sample processing was performed on a FACSCanto II (BD Biosciences) and with FlowJo 10 software (Tree Star). The fraction of total activated cells was calculated as the percentage of $CD25^+CD69^+$ cells out of the total singlet, viable $CD5^+$ lymphocytes. Means of four replicates with s.d. were calculated. The T cell activation assay was repeated five times. For microscopic analysis, PA-1/luc cells were electroporated with 20 µg/ml CD3 × CLDN6 or PLAC1 × CD3 (irrelevant target) bi-$(scFv)_2$ IVT mRNA. Unstimulated human T cells enriched by magnetic sorting were co-cultured with electroporated target cells at an E:T ratio of 5:1. The assay was performed in transparent 48-well plates and repeated three times. Images were acquired at ×200 magnification with an Olympus IX53 inverted microscope after 24 h of incubation.

Immunohistochemistry. Xenografts from PBMC humanized mice were fixed in 4% formalin and embedded in paraffin. 4-µm sections were cut from each FFPE block and incubated 1 h at 58 °C before deparaffinization. FFPE sections were boiled in 10 mM citric acid supplemented with 0.05% Tween-20 (pH 6.0) at 120 °C for 10 min. Endogenous peroxidases were quenched by incubation in 0.3% H_2O_2 in PBS for 15 min. After washing with PBS, nonspecific antibody-binding sites were blocked with blocking solution (10% goat serum in PBS) and sections were incubated overnight with the specific primary antibody diluted in blocking buffer. For detection of $CD3^+$ tumor-infiltrating lymphocytes and analysis of CLDN6 expression, sections were stained with monoclonal anti-CD3 antibody (clone SP7; ab16669, Abcam) or polyclonal anti-CLDN6 antibody (18865, IBL). Visualization was performed via incubation with HRP-conjugated secondary antibody (polyclonal HRP-conjugated anti–rabbit IgG antibody, ImmunoLogic) for 30 min at room temperature followed by addition of the corresponding peroxidase substrate (Vector Nova Red, Vector Laboratories). After counterstaining with hematoxylin, dehydration and mounting, the sections were scanned using the Axio Scan.Z1 (Zeiss) to obtain high-resolution digital images and analyzed microscopically for CLDN6 expression. Manually predefined tumor areas on CD3-stained sections were quantified via computerized image analysis software (Tissue Studio 4.2, Definiens Developer XD 64 2.5.0).

Bioluminescence imaging. Uptake and translation of luciferase mRNA were evaluated in female BALB/cJRj mice (aged 6–8 weeks) by *in vivo* bioluminescence imaging using the Xenogen IVIS Spectrum imaging system (Caliper Life Sciences). An aqueous solution of l-luciferin (250 µl, 1.6 mg; BD Biosciences) was injected i.p. 6 h after i.v. injection of 5 µg of luciferase mRNA complexed with the TransIT-mRNA transfection kit (further imaging was performed every 24 h after i.v. injection of the mRNA complexes). Emitted photons from live animals were quantified 10 min later with an exposure time of 1 min. Regions of interest were quantified as the average radiance (photons per second per cm^2 per steradian; represented by color bars) using IVIS Living Image 4.0 software.

Pharmacokinetic profile. NSG mice were injected i.v. with 5 µg of TransIT-formulated luciferase control mRNA or CD3 × CLDN6 bi-$(scFv)_2$ mRNA or with 4–7 µg (200 µg/kg body weight) purified rCD3 × CLDN6 protein. Blood samples were taken from the periorbital venous sinus at indicated time points (first bleeding of protein-treated mice 15 min after injection and of mRNA-treated

mice 30 min after injection). Blood was collected in lithium-heparin microvettes (Sarstedt) and centrifuged at 4,000 rpm at room temperature for 5 min. Plasma was aliquotted, shock frozen and stored at −65 to −85 °C until analysis.

Mouse xenograft models. NSG mice (male and female, aged 7–18 weeks) were implanted subcutaneously in the upper right flank with 5×10^6 OV-90 or 3×10^6 ES-2 (WT) or ES-2/hCLDN6 tumor cells. 6–8 d before the start of treatment, 1×10^7 PBMCs were administered i.p. and their engraftment was verified via staining with anti-CD45-APC (clone HI30; 555485, BD Bioscience) of peripheral blood by flow cytometry. Mice were randomized according to tumor size into mixed-sex treatment groups. Treatment was conducted with 3 µg (OV-90) or 5 µg (ES-2) of TransIT-formulated luciferase control mRNA or CD3 × CLDN6 or EpCAM × CD3 bi-$(scFv)_2$ mRNA by i.v. injection via the retro-orbital venous plexus. As a positive control, 200 µg/kg body weight purified rCD3 × CLDN6 protein[15] or rEpCAM × CD3 protein was injected i.p. three times (rCD3 × CLDN6 protein) or i.v. once (rEpCAM × CD3 protein) per week. Proteins in 10 mM NaOAc, pH 5.5, vehicle buffer and the vehicle itself were supplemented with glucose to a final concentration of 5% for injections.

Tumors were measured without blinded to treatment with a digital caliper twice weekly, and volumes were calculated by the formula tumor volume (mm^3) = length (mm) × (width (mm))^2/2. Termination criteria were a tumor volume of 1,500 mm^3 or weight loss of 20% due, for example, to graft-versus-host (GvH) reaction. No mice were excluded from study analyses.

Human and mouse cytokine detection. Concentrations of human IFN-γ, IL-1β, IL-6 and TNF-α were determined via the V-PLEX Human Proinflammatory Panel 1 (4-Plex) kit according to the manufacturer's protocol (Meso Scale Discovery) and analyzed on a Meso QuickPlex SQ 120 reader. Lithium-heparin plasma from NSG mice was used at a 1:2 dilution.

Mouse IFN-α and TNF-α concentrations were analyzed in undiluted serum from BALB/cJRj mice according to the manufacturer's protocols for Mouse IFN-α Platinum ELISA and Mouse TNF-α ELISA Ready-SET-Go! (Affymetrix/eBioscience). The limit for quantification was 8 pg/ml.

Clinical chemistry analysis. The ALT and AST transaminases and lactate dehydrogenase (LDH) were analyzed in serum from female BALB/cJRj mice diluted 1:2 in water (total of 100 µl) by the Indiko Clinical and Specialty Chemistry System (Thermo Scientific). Reference ranges for the parameters were determined with serum samples from >30 untreated BALB/cJRj mice.

Statistical analyses and data presentation. Statistical analyses were performed in GraphPad Prism 6 software. Results are expressed as means ± s.d. or medians with or without interquartile ranges. Biological replicates such as different cell passages, effector cell preparations and RiboMAB preparations were used in all *in vitro* studies. *In vivo* studies were performed once unless stated otherwise. The D'Agostino & Pearson omnibus was used as a normality test. Parametric group comparisons were performed by unpaired two-tailed Student's *t* test (with a preceding *F* test to compare the variances of the two groups tested), and statistically significant findings for *in vitro* assays were in addition confirmed by execution of at least three independent experiments. Non-parametric or group comparisons with small sample sizes were assessed by unpaired two-tailed Mann–Whitney *U* test. Differences in median tumor growth data (**Fig. 2d,e** and **Supplementary Fig. 4a**) were assessed by parametric two-way ANOVA. Multiple comparisons were addressed by parametric two-way ANOVA in combination with Tukey's test (**Fig. 1d**) or by multiple *t* test with correction for multiple comparisons using the Holm–Sidak method (**Supplementary Fig. 5c**). $P < 0.05$ was considered statistically significant for all tests: ns, $P \geq 0.05$, $^*P \leq 0.05$, $^{**}P \leq 0.01$, $^{***}P \leq 0.001$, $^{****}P \leq 0.0001$. No statistical method was used to predetermine sample size for animal or other experiments.

Data availability. The data that support the findings of this study are available from the corresponding author upon reasonable request.

16. Sahin, U., Türeci, Ö., Brandenburg, G. & Usener, D. US patent 8,425,902 (2013).
17. Sahin, U. *et al.* US patent 9,487,584 (2016).
18. Roovers, R.C. *et al. Br. J. Cancer* **78**, 1407–1416 (1998).
19. Lanzavecchia, A. & Scheidegger, D. *Eur. J. Immunol.* **17**, 105–111 (1987).
20. Traunecker, A., Lanzavecchia, A. & Karjalainen, K. *EMBO J.* **10**, 3655–3659 (1991).
21. Gallie, D.R., Tanguay, R.L. & Leathers, V. *Gene* **165**, 233–238 (1995).
22. Vallazza, B. *et al. Wiley Interdiscip. Rev. RNA* **6**, 471–499 (2015).

doi:10.1038/nm.4356

Erratum: Elimination of large tumors in mice by mRNA-encoded bispecific antibodies

Christiane R Stadler, Hayat Bähr-Mahmud, Leyla Celik, Bernhard Hebich, Alexandra S Roth, René P Roth, Katalin Karikó, Özlem Türeci & Ugur Sahin

Nat. Med. **23, 815–817 (2017); published online 12 June 2017; corrected after print 20 July 2017**

In the version of this article initially published, in the "Polymer/lipid-based formulation of mRNA" section of the Online Methods, the text incorrectly stated that mRNA was in 190 ml rather than 190 μl of cold DMEM. The error has been corrected in the HTML and PDF versions of the article.